Broadband Sparse Sensing: A Polynomial Matrix Approach to Co-Prime and Super Nested Arrays

William Coventry, Carmine Clemente, and John Soraghan
University of Strathclyde, CESIP, EEE, 204, George Street, G1 1XW, Glasgow, UK
E-mail: william.coventry, carmine.clemente, j.soraghan- @strath.ac.uk

***Abstract*—Passively monitoring the spectrum for detection and localisation of radar sources is ever more fraught with difficulty due to the advent of low probability of intercept (LPI) radar technology. A key aspect of LPI radar waveform design are the spread spectrum modulation schemes, instead of concentrating power over a narrow- bandwidth, this power can be spread across a broad-bandwidth making the source difficult to detect using conventional ESM methods. Such sources prompt the need for new detection, and direction of arrival estimation methods. Moreover, broadband antennas and their subsequent processing systems are expensive in terms of both cost and power - forcing a real world feasible limit on the number of antennas in a system. In addition, a fine spacing is required for ambiguity free direction of arrival estimation of higher frequency sources while a wide aperture is required for sufficient resolution of lower frequency sources. In this paper we present a novel sparse broadband direction of arrival method based upon co-prime and super-nested array geometries, using polynomial matrix methods whereby a new virtual array is formed containing many more virtual elements than in the physical array.**

I. Introduction

Radar systems may utilise a broadband modulation scheme for enhanced resolution capabilities [1], or alternatively to avoid detection. A key characteristic of LPI radar waveforms is spreading energy in both time and frequency [2]. By spreading the energy of a pulse over time and frequency, the peak power of the LPI waveform is low as compared to a conventional radar system, reducing its probability of interception. Thus to detect and locate such a source, a broadband direction of arrival method could be utilised.

It has been shown that polynomial matrices provide an attractive solution for broadband array processing problems, such as detection, beamforming [3] and direction of arrival estimation [4]. Other methods of broadband direction of arrival involve coherent signal subspace methods [5],[6] whereby the covariance matrices at each frequency bin are focussed onto a single covariance matrix at the centre frequency. Such methods however may be inappropriate in applications such as passive monitoring, as there may be many sources of varying carriers and bandwidths.

Spatial sparse sensing methods have gained significant interest in recent years owing to the fact that up to $O(N^2)$ degrees of freedom can be gained from just $O(N)$ sensors [7]. One method aiming to achieve such an increase is the minimum redundancy array (MRA) [8]. However, calculating the positions of these sensors is difficult task due to the MRA having no closed form expression, and is thus not considered in this paper.

Two popular sparse geometries are co-prime [9] and nested arrays [7] as these have simple closed form expressions and calculating sensor positions for arbitrary N is a problem of easy solution. Nested arrays are the union of two uniform linear sub-arrays; a dense Nyquist spaced uniform linear array (ULA), and a sparse ULA. Such geometry yields a hole-free co-array, but there are practical issues due to the dense ULA, such as manufacturing difficulties and mutual coupling between adjacent elements [10].

The co-prime array is also the union of two uniform linear sub-arrays, and has exactly only two pairs of sensors at this Nyquist spacing - but the co-array contains holes. The holes in the co-array present difficulties in methods such as the co-array MUSIC [11], and thus only the uniform section of this co-array can be utilised, decreasing the overall degrees of freedom which can be exploited.

More recently, a modified version of the nested array has been introduced; the super nested array [10]. Such an array has the advantages of the conventional nested array, however by redistributing the dense elements along the array aperture, there are significantly less sensors at Nyquist spacing, relieving the array design of mutual coupling effects.

The remainder of the paper is structured as follows: Section II discusses some properties and definitions of sparse arrays, and introduces the co-prime, nested, and super nested array geometries. Section III discusses the data model for broadband sources illuming an antenna array. Polynomial matrices, the formation of the Polynomial based virtual linear array, and the idea of spatial smoothing based decorrelation with polynomial matrices is covered in Section IV. Section V analyses the performance of the super nested, and co-prime array geometries in the sense of broadband direction of arrival estimation, and is compared to a ULA of similar aperture. Finally, Section VI summarises the paper, and provides ideas for future work in this area.

Notation: vectors and matrices are denoted by bold lower- and upper case variables, e.g. $\boldsymbol{a}$ and $\boldsymbol{A}$. Polynomial matrices are represented by the suffix of (z), and the super script P denotes the parahermitian operator of a polynomial vector or matrix, and is defined as $A^P(z) = A^H(z^{-1})$.

II. Sparse Arrays

Consider a set N of sensors placed on a uniform linear grid of spacing $d = \lambda_{\text{min}}/2$, λ_{min} being the wavelength of the highest frequency source to illuminate the array ensuring unambiguous angle determination for all angle of arrival. The sensor x_n is placed at the physical location nd. The key to sparse sensing is the difference set, defined as:

$$D = \{x_i - x_j\}, \forall i, j = 0, 1, \ldots, N-1 \tag{1}$$

This is a peer-reviewed, accepted author manuscript of the following conference paper:
Coventry, W., Clemente, C., & Soraghan, J. (2019). Broadband sparse sensing: a polynomial matrix approach to co-prime and super nested arrays. In 2019 IEEE Radar Conference [8835665] Institute of Electrical and Electronics Engineers Inc.. https://doi.org/10.1109/RADAR.2019.8835665

The significance of this difference set is that it defines which spatial lags the second order statistics can be estimated at, which arises naturally when estimating a spatial covariance matrix:

$$\boldsymbol{R}_{xx}(\tau) = E[\boldsymbol{x}(n)\boldsymbol{x}^H(n-\tau)] \tag{2}$$

where τ denotes the temporal lag parameter, which is often only considered for $\tau = 0$ in narrowband applications, and $\boldsymbol{x}(n)$ is the sampled array vector: $\boldsymbol{x}(n) = [x_0(n), x_1(n) \ldots, x_N(n)]^T$. As an example, lets explore the weight function of the difference set of a uniform linear array of $N = 21$ sensors. The weight function $w(u)$ is defined as the number of times the spatial lag u occurs in the difference set.

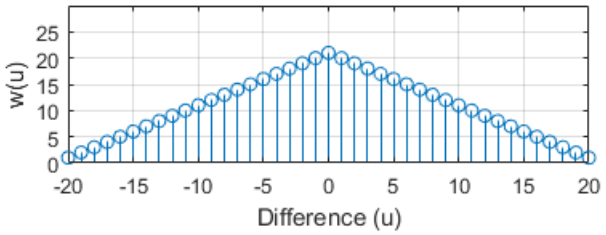

Figure 1: Difference set Weights for a 21 Element ULA

The cardinality of the unique elements in difference set defines the degrees of freedom (DoF) in an array geometry. In the case of a uniform linear array, there are $2N + 1$ freedoms in its difference set - with high weights for u, Figure 1 demonstrates the weight function of a 21 elements ULA. If a difference occurs more than once, then this implies a loss in cardinality and thus a decrease in DoF.

A. Co-Prime Array

The extended co-prime array geometry seen in Figure 2, initially proposed in [11] involves the union of two uniform linear arrays; one array being S_n, where there are N sensors with Md spacing, and the other being S_m, where there $2M$ sensors with Nd spacing, where M and N are co-prime integers. Owing to this co-primality, they only share a sensor at position 0, and there are thus $2M + N - 1$ physical sensors overall. As an example, lets consider the weight function of a co-prime array where $M = 3$ and $N = 4$. Figure 3 shows

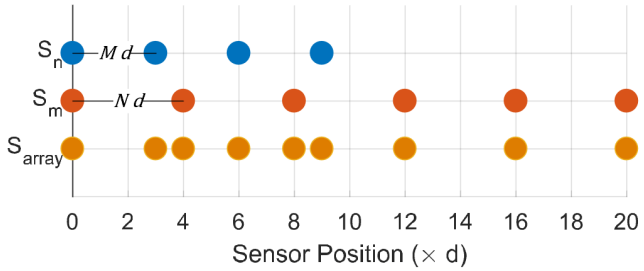

Figure 2: Extended co-prime array geometry for M=3,N=4

the weight function for the array geometry in Figure 2. It can be seen that there are 35 distinct elements in the difference co-array, however there are 'holes' in this difference co-array

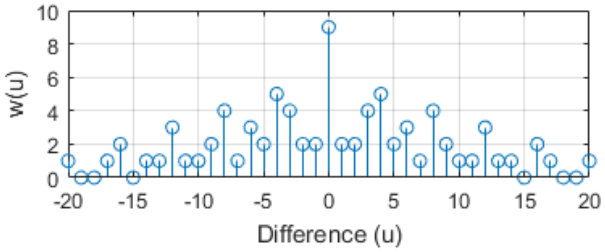

Figure 3: Weight Function for M=3,N4 Co-Prime Array

and it is only contiguous in the region $-(MN + M - 1)$ to $(MN + M - 1)$ for reasons stated in Section IV, the method used in this paper requires a hole-free co-array, with this extended co-prime array geometry, only $2(MN + M) - 1$ uniform degrees of freedom can be exploited.

B. Nested Array

Similarly to the co-prime array, the nested array is also based upon two uniform arrays [7]. The first ULA is densely spaced with N_1 sensors spaced at d, and a sparse array with N_2 sensors spaced at $(N_1+1)d$ over an aperture of $N_2(N_1+1)d$, utilising $N_1 + N_2$ sensors overall. The geometry of such and array can be seen in Figure 4, and its weight function can be seen in Figure 5

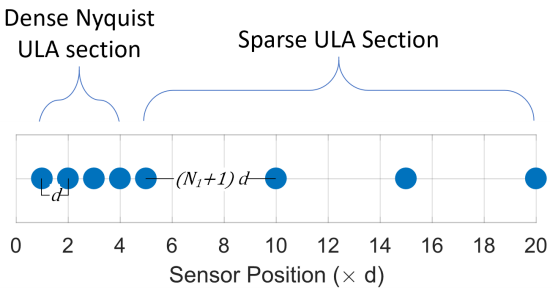

Figure 4: Nested Array Geometry

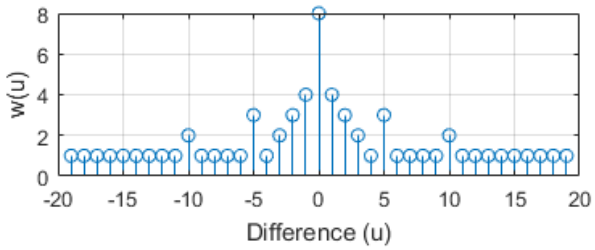

Figure 5: Weight Function for the Nested Array

This geometry might have a slightly smaller aperture but it has one less sensor and it contains a hole free difference co-array, yielding $2(N_2(N_1 + 1))$ uniform DoF. For traditional arrays it well known that the physical aperture determines the resolution and accuracy of the estimator, however in sparse arrays this is determined by the uniform DoF [10].

However, due to the dense Nyquist spaced ULA practical

issues may arise in such array geometries - such as difficulties in manufacturing and mutual coupling between adjacent sensors [10].

1) Super-Nested Array: Super nested arrays alleviate these practical issues by redistributing the dense elements along the entire array aperture, without affecting the attractive large contiguous region of the conventional nested array, whilst minimising the number of sensors spaced at distance d. By utilising the method described in [10], a second order super nested array for $N_1 = N_2 = 4$ is formed with the array geometry displayed in Figure 6

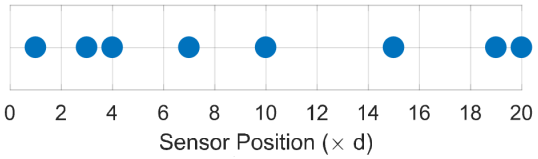

Figure 6: Super Nested Array Geometry

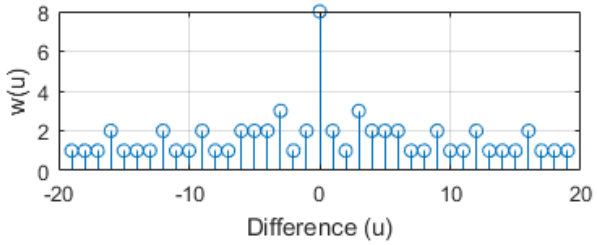

Figure 7: Weight Function for the 2^{nd} Super Nested Array

The weight function of the super nest in figure 7 has the same cardinality of the conventional nested array, but with reduced weights at Nyquist spacing, d ($w(1)$ and $w(-1)$). Thus this super nested array boasts the advantages of the conventional, with less sensors spaced at Nyquist. The effect of mutual coupling can be reduced even further by utilising higher order super-nested arrays [12]

III. Data Model

If a source is narrowband, then the time period of its complex envelope is significantly greater than the time it takes the wave front to traverse the array. Owing to this narrowband approximation, the signal seen at each antenna element is a phase shifted version at the carrier frequency, yielding a relatively simple instantaneous mixture model. For broadband sources, such an approximation is invalid, and the inter-element delay must be modelled as a linear phase shift across all frequencies. This motivates the following convolutive mixture model:

$$\boldsymbol{x}(n) = \sum_{l=1}^{L} [\boldsymbol{a_l} \odot s_l(n)] + \boldsymbol{\nu}(n) \tag{3}$$

where there are L uncorrelated sources present, $\boldsymbol{x}(n)$ is the received signal vector at sample index n, $\boldsymbol{a}_l$ is the broadband steering vector of the l^{th} source, comprising of ideal fractional delay FIR filters [13], $s_l(n)$ the l^{th} source signal, and $\boldsymbol{\nu}(n)$ is the noise vector, which is assumed to be uncorrelated Gaussian and spectrally white.

Consider the case where S_{ai} denotes the position of the i^{th} sensor in the set S_a, and placed on a linear grid of spacing $\lambda_{\min}/2$, i.e. half the wavelength of the highest frequency expected. The broadband steering takes the form:

$$\boldsymbol{a_l}(k) = \begin{bmatrix} \delta[k - S_{a1}\tau_l] \\ \delta[k - S_{a2}\tau_l] \\ \vdots \\ \delta[k - S_{aN}\tau_l] \end{bmatrix} \tag{4}$$

where $\delta[k - \tau]$ represents the ideal fractional delay filter for delay τ (in samples), and τ_l represents the inter-element delay at Nyquist spacing, and is the parameter dependant on the direction of arrival such that $\tau_l = d\sin(\theta_l)/cT_s$, with θ_l being the l^{th} source's direction of arrival, and T_s being the temporal sample period.

IV. Polynomial Matrix Approach

For both the co-prime and super nested array, the method of forming the virtual array remains the same, and is covered in this section. The motivation behind polynomial matrices lies within the convolutive mixture model from (3), since considering only instantaneous ($\tau = 0$) temporal correlations is now insufficient. It is now appropriate to consider a range of temporal correlations in addition to the spatial, and thus the definition of the following space time covariance matrix:

$$\boldsymbol{R_{xx}}(z) = \sum_{\tau=-\infty}^{\infty} \boldsymbol{R_{xx}}(\tau) z^{-\tau} \tag{5}$$

where $\boldsymbol{R}_{xx}(\tau) = E[\boldsymbol{x}(n)\boldsymbol{x}^H(n-\tau)]$ and is the covariance matrix at lag τ, and $\boldsymbol{R}_{ss}(\tau) = E[\boldsymbol{s}(n)\boldsymbol{s}^H(n-\tau)]$ is the source covariance matrix, which will be diagonal for uncorrelated sources. Since this is assumed, this polynomial space time covariance may be expressed as:

$$\boldsymbol{R}_{xx}(z) = \sum_{l=1}^{L} [\sigma_l^2(z)\boldsymbol{a}_l(z)\boldsymbol{a}_l^P(z)] + \sigma_n^2\boldsymbol{I} \tag{6}$$

where $\sigma_l^2(z)$ represents the autocorrelation function of the l^{th} source, and σ_n^2 is the noise variance.

Recall the elements of the matrix contain all spatial differences for sensor positions, i.e the component $\langle \boldsymbol{R}_{xx}(z) \rangle_{ij}$ represents the spatial auto- (for $i = j$) and cross-(for $i \neq j$) correlations for spatial difference $i - j$, thus the space-time covariance matrix contains correlations at all lags within the difference set and by vectorising this matrix, a virtual array with positions contained in the difference set is obtained.

$$\boldsymbol{\gamma}(z) = \text{vec}(\boldsymbol{R}_{xx}(z)) \tag{7}$$

where $\boldsymbol{\gamma}(z)$ is the virtual array. From the weight functions in Figures 3 and 7, it can be seen that there are 'repeating' elements of this virtual array, i.e. $w(u) > 1$. These repeating elements are often referred to as redundant - but they can be averaged into one virtual array sensor to potentially improve the estimate of the correlation at that specific virtual sensor. In reality, this may make little difference assuming a good

estimate of $\boldsymbol{R}_{xx}(z)$ to begin with. This virtual array vector may also be represented as:

$$\boldsymbol{\gamma}(z) = \text{vec}\Big[\sum_{l=1}^{L}[\sigma_l^2(z)\boldsymbol{a}_l(z)\boldsymbol{a}_l^P(z)]\Big] + \sigma_n^2\tilde{\mathbf{1}} \tag{8}$$

where $\tilde{\mathbf{1}}$ is the diagonalised identity matrix, i.e. a vector of zeros, with ones at the positions denoting spatial autocorrelations. Here, it can be reformulated into a more familiar array processing problem:

$$\boldsymbol{\gamma}(z) = \boldsymbol{B}(z)\tilde{\boldsymbol{s}}(z) + \sigma_n^2\tilde{\mathbf{1}} \tag{9}$$

where $\boldsymbol{B}(z)$ is the steering vector of the much larger virtual array, and is:

$$\boldsymbol{B}(z) = [\boldsymbol{a}_1^*(z) \otimes \boldsymbol{a}_1(z) \dots \boldsymbol{a}_L^*(z) \otimes \boldsymbol{a}_L(z)]^T \tag{10}$$

and $\tilde{\boldsymbol{s}}(z)$ is the source vector, containing the autocorrelation functions of the L sources illuminating the array.

$$\tilde{\boldsymbol{s}}(z) = [\sigma_1^2(z), \sigma_2^2(z) \dots \sigma_L^2(z)] \tag{11}$$

Since the new source vector contains the autocorrelation functions, the matrix $\tilde{\boldsymbol{s}}(z)\tilde{\boldsymbol{s}}^P(z)$ will be singular, and thus all sources will appear correlated.

A. Spatial Smoothing

A well known method of effectively restoring the rank of the source covariance matrix is spatial smoothing, recently extended to broadband scenarios via polynomials in [14]. Since this method exploits the translational invariance of sub-arrays, it is limited to array structures whereby the steering vector has a Vandermonde structure, such as a uniform linear array.

Hence the virtual linear array from (9) must be truncated and rearranged such that it is now a virtual uniform linear array, i.e.

$$\boldsymbol{\gamma}_1(z) = \boldsymbol{A}_1(z)\tilde{\boldsymbol{s}}(z) + \sigma_n^2\tilde{\boldsymbol{e}} \tag{12}$$

where $\boldsymbol{A}_1(z)$ is the broadband steering matrix for the virtual linear array, and $\tilde{\boldsymbol{e}}$ is a vector of zeros, with a one at the virtual array position zero. In order to detect G coherent sources, the virtual uniform linear array should be split into G overlapping subarrays. However, we assume that the number of sources are not known a priori - thus with no prior knowledge of the number of sources, it is sensible to utilise half the virtual aperture to ensure decorrelation. In the case of the co-prime array this would involves $D = MN + M - 1$ overlapping subarrays containing D elements, and for the super nested virtual array this would involve $D = N_2(N_1 + 1) + 1$. The virtual uniform linear array vector at the i^{th} subarray takes the form:

$$\boldsymbol{\gamma}_{1i}(z) = \boldsymbol{A}_{1i}(z)\tilde{\boldsymbol{s}}(z) + \sigma_n^2\tilde{\boldsymbol{e}}_i \tag{13}$$

and thus the space-time covariance at the i^{th} subarray:

$$\boldsymbol{R}_i(z) = \boldsymbol{\gamma}_{1i}(z)\boldsymbol{\gamma}_{1i}^P(z) \tag{14}$$

The mean covariance matrix yields the spatially smoothed space-time covariance matrix, which will be positive semidefinite for all lags [15].

$$\hat{\boldsymbol{R}}_{xx}(z) = \frac{1}{D}\sum_{i=1}^{D}\boldsymbol{R}_i(z) \tag{15}$$

The resulting polynomial matrix will yield an L dimensional signal subspace, and can thus be used for subspace based methods, such as the polynomial MUSIC algorithm [4], or the polynomial root-MUSIC algorithm [16] for computational advantages.

V. Performance Analysis

In this section we compare the direction of arrival estimation capabilities of the co-prime, super nested and uniform linear arrays of equal physical aperture . To anlalyse this, we utilise the SMD-PEVD [17] [18], polynomial MUSIC, and the polynomial root-MUSIC algorithms.

A. Polynomial Eigenvalue Decomposition

Similarly to a conventional eigenvalue decomposition, the space time covariance matrix can be decomposed into its polynomial eigenvalues and paraunitrary eigenvectors:

$$\boldsymbol{R}_{\boldsymbol{xx}}(z) = \boldsymbol{U}(z)\boldsymbol{\Lambda}(z)\boldsymbol{U}^P(z) \tag{16}$$

Whereby the polynomial eigenvalue power spectral density:

$$\boldsymbol{\Lambda}(e^{j\Omega}) = \text{diag}[\boldsymbol{\Lambda}_1(e^{j\Omega}), \boldsymbol{\Lambda}_2(e^{j\Omega}), \dots, \boldsymbol{\Lambda}_L(e^{j\Omega})] \tag{17}$$

is spectrally majorised such that $\boldsymbol{\Lambda}_1(e^{j\Omega}) > \boldsymbol{\Lambda}_2(e^{j\Omega}) > \dots > \boldsymbol{\Lambda}_L(e^{j\Omega})$. Similarly to conventional eigenvalues, the number of significant polynomial eigenvalues determines the dimensions of the signal, and noise subspaces, and thus the number of sources, hence (16) can be partitioned such that

$$\boldsymbol{R}_{\boldsymbol{xx}}(z) = [\boldsymbol{U}_{\boldsymbol{s}}(z) \quad \boldsymbol{U}_{\boldsymbol{n}}(z)] \begin{bmatrix} \boldsymbol{\Lambda}_{\boldsymbol{s}}(z) & \\ & \boldsymbol{\Lambda}_{\boldsymbol{n}}(z) \end{bmatrix} \begin{bmatrix} \boldsymbol{U}_{\boldsymbol{s}}{}^P(z) \\ \boldsymbol{U}_{\boldsymbol{n}}{}^P(z) \end{bmatrix} \tag{18}$$

and this algorithms such as Polynomial MUSIC and Polynomial Root-MUSIC can be performed.

B. Spatio-Spectrum Estimation

The spatio spectrum is estimated via the polynomial MUSIC algorithm:

$$P_{mu}(\theta, \Omega) = \frac{1}{\boldsymbol{a}_\theta^P(z)\boldsymbol{U}_n(z)\boldsymbol{U}_n^P(z)\boldsymbol{a}_\theta(z)}|z = e^{j\Omega} \tag{19}$$

This spatio-spectrum contains information on the direction of arrival of all L sources, in addition to their frequencies. Figure 8 shows the performance of the spatio-spectrum estimation at a 0 dB SNR. The ground truth of the sources can be seen in Table I.

Table I: Simulation Parameters

Source No.	Normalised frequencies (rad/s)	DoA (°)
1	$\Omega \in [0.50\ 0.80]\pi$	$\theta = -65$
2	$\Omega \in [0.40\ 0.80]\pi$	$\theta = -43.3$
3	$\Omega \in [0.51\ 0.81]\pi$	$\theta = -21.7$
4	$\Omega \in [0.45\ 0.71]\pi$	$\theta = 0$
5	$\Omega \in [0.53\ 0.83]\pi$	$\theta = 21.7$
6	$\Omega \in [0.34\ 0.62]\pi$	$\theta = 43.3$
7	$\Omega \in [0.47\ 0.75]\pi$	$\theta = 65$

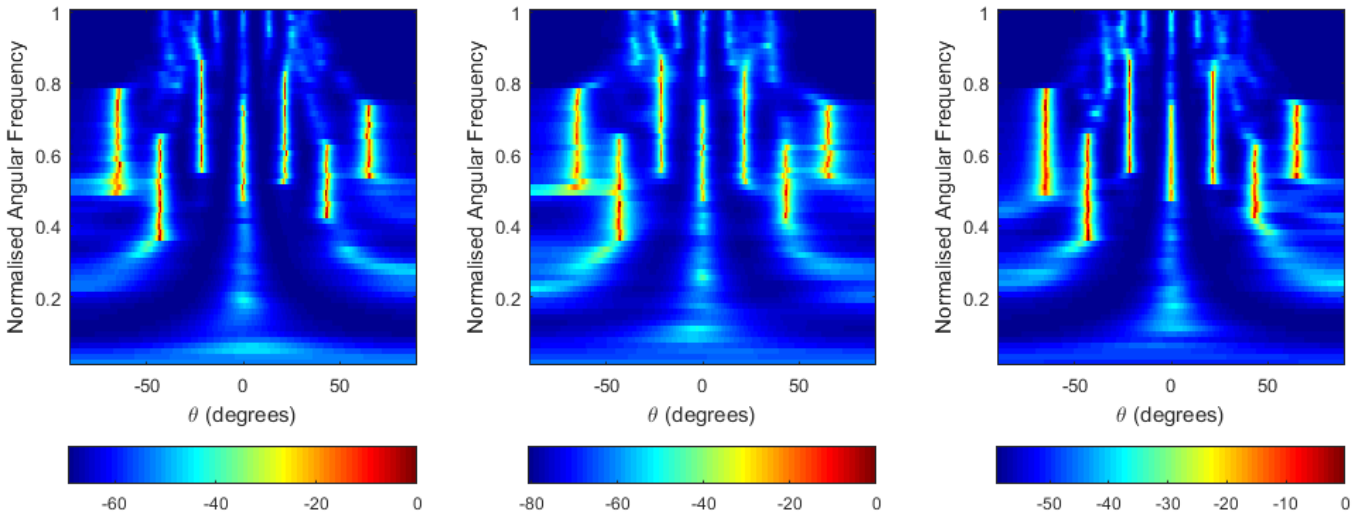

(a) Second Order Super Nested Array, $N_1 = N_2 = 4$ and thus 8 elements overall

(b) Extended Co-Prime array - $M = 3, N = 4$ and thus 9 elements overall

(c) 21 Element Uniform Linear Array

Figure 8: Spatio-Spectrum Estimation for super nested, co prime and uniform linear arrays. The ground truth frequency and DoA parameters can be seen in Table I

C. Probability of Resolution

The probability of resolving two sources spaced at $\Delta\theta = \theta_1 - \theta_2$ is found empirically in this section, using the spatial only function of the polynomial MUSIC algorithm:

$$P_{mu}(\theta) = \sum_{i=N_{fl}}^{N_{fh}} P_{mu}(\theta, e^{j\Omega_i}) \tag{20}$$

where N_{fl} and N_{fh} are the lowest and highest frequency bins which contain significant energy. The sources are said to be resolved if the following criteria is met:

$$P_{mu}(\Delta\theta) \leq \frac{1}{2}[P_{mu}(\theta_1) + P_{mu}(\theta_2)] \tag{21}$$

Beyond this point, the spectrum starts to merge into one peak, making the sources unresolvable [19]. Thus the probability of resolution for a single run:

$$P_r(\Delta\theta) = \begin{cases} 1 & \text{if } P_{mu}(\Delta\theta) \leq \frac{1}{2}[P_{mu}(\theta_1) + P_{mu}(\theta_2)] \\ 0 & \text{otherwise} \end{cases} \tag{22}$$

A Monte Carlo simulation of 100 runs per $\Delta\theta$ is performed with two identical sources, temporally separated such that there is no overlap with normalised bandwidth of $\Omega \in [0.5\pi\ 0.8\pi]$ rad/s at 10 dB SNR. The mean probability of resolution can be seen in Figure 9. While all array geometries have a very similar aperture, their uniform DoF vary - with the 21 element ULA having 21 uniform freedoms, the $N_1 = N_2 = 4$ super nested array having $N_2(N1 + 1) = 20$ freedoms (after spatial smoothing), with only 8 overall sensors, and the $N = 4, M = 3$ co prime array having only $MN + M - 1 = 14$ freedoms (after spatial smoothing). This is reflected via the differences in resolution in Figure 9. While it is easy to see that the dense ULA outperforms both sparse arrays, it is worth noting that the

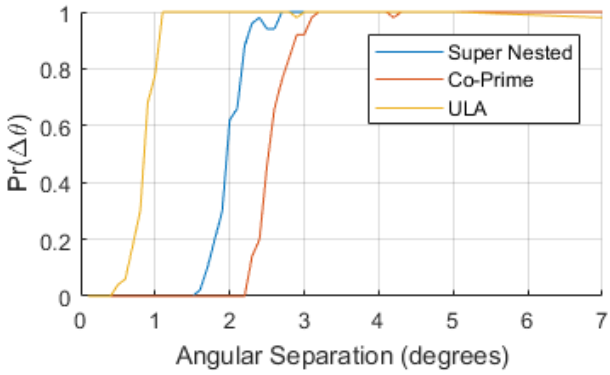

Figure 9: Probability of Resolution at 10 dB SNR

super nested array utilises only 38% of the sensors of the ULA, and 42% for the co-prime. Clearly, this significant reduction in the number of sensors comes at a cost of resolution in this simulation.

D. Accuracy

In order to compare the estimation accuracy using all three array geometries, A Monte-Carlo simulation of $I = 100$ runs over a range of SNRs with a single source of fixed bandwidth source, where the DoA is randomised for each run. For reduced computation, the Polynomial Root-MUSIC algorithm [16] is used. To compare the accuracy of the three geometries, the mean squared error is analysed:

$$RMSE = \sqrt{\sum_{i=1}^{I} [\hat{\theta}_i - \theta]^2} \tag{23}$$

where $\hat{\theta}$ is the estimated DoA from the Polynomial Root-MUSIC algorithm, and θ is the ground truth DoA. The results can be seen in Figure 10 While all geometries perform well

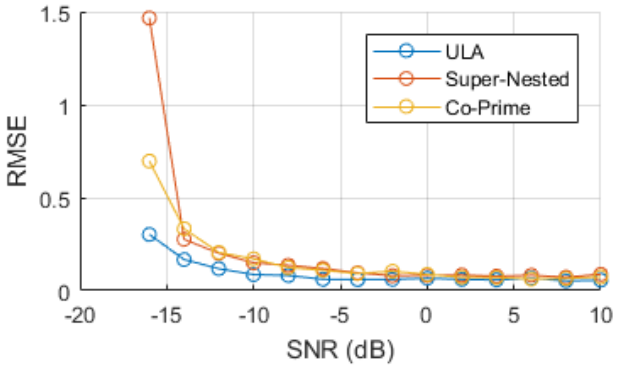

Figure 10: Accuracy Comparison between the uniform, super nested and co-prime arrays

at most SNRs, the super-nested array performs slightly worse than the ULA of similar aperture but vastly more elements, yet outperforms the co-prime geometry. This is expected due to the differences in uniform DoF, as mentioned in Section V-C

Lets consider the following scenario to add some perspective to these results. A source placed 10 km from the receiver and the received SNR is 0 dB. From Figure 10 the RMSE of the DoA capability of the ULA, super-nested and co-prime arrays are $0.07°$, $0.08°$ and $0.09°$ respectively. Thus for the location capabilities of these geometries of the source at 10 km, the errors would be roughly ± 6 m, ± 7 m and ± 8 m. Now assuming a 10 dB received SNR, from Figure 9, for a 90% chance of resolving sources, the minimum $\Delta\theta$ is $1°$, $2.2°$ and $2.9°$ for the ULA, super-nested and co-prime geometries. For the aforementioned scenario with an additional source of identical bandwidth, the minimum distance between the two sources for them to be resolvable would be 174 m, 384 m, and 506 m. While the ULA here does have the smallest error in location estimation and smallest resolution angle, it is worth remembering that this geometry utilises 13 more sensors than the nested, and 12 more than the co-prime.

VI. Conclusion

In summary, we have extended the super-nested and co-prime sparse array geometries to broadband scenarios via the use of polynomial matrices to form the polynomial virtual linear array. The performance of the spatio-spectrum, probability of resolution and accuracy of the array geometries is analysed using both the Polynomial MUSIC, and Polynomial Root MUSIC algorithms. It is clear that in the presented scenarios, the super-nested array outperforms the co-prime array whilst utilising one less sensor owing to the greater uniform degrees of freedom in the co-array, and performs close to a 21 element uniform linear array whilst utilising 61% fewer sensors. Future work in this area involves research alternate methods of decorrelation such that less virtual aperture is spent on the spatial smoothing step, which could potentially improve results further.

Acknowledgment

This work was supported by Leonardo MW Ltd and EPSRC grant number EP/N509760/1.

References

[1] M. A. Richards, W. A. Holm, and J. A. Scheer, *Principles of Modern Radar*. Scitech Publishing, 2010.

[2] P. E. Pace, *Detecting and Classifying Low Probability of Intercept Radar*. Artech House, 2008.

[3] S. Weiss, S. Bendoukha, A. Alzin, F. K. Coutts, I. K. Proudler, and J. Chambers, "MVDR BROADBAND BEAMFORMING USING POLYNOMIAL MATRIX TECHNIQUES Department of Electronic & Electrical Engineering , University of Strathclyde , Glasgow , Scotland Department of Electrical Engineering , College of Engineering , Taibah University , Yanbu , Sa," pp. 844–848, 2015.

[4] M. A. Alrmah, S. Weiss, and S. Lambotharan, "An extension of the music algorithm to broadband scenarios using a polynomial eigenvalue decomposition," in *2011 EUSIPCO*, Aug 2011, pp. 629–633.

[5] H. Wang and M. Kaveh, "Coherent signal-subspace processing for the detection and estimation of angles of arrival of multiple wide-band sources," *IEEE Transactions on Acoustics, Speech, and Signal Processing*, vol. 33, no. 4, pp. 823–831, August 1985.

[6] P. Pal and P. P. Vaidyanathan, "A novel autofocusing approach for estimating directions-of-arrival of wideband signals," in *2009 Conference Record of the Forty-Third Asilomar Conference on Signals, Systems and Computers*, Nov 2009, pp. 1663–1667.

[7] ——, "Nested arrays: A novel approach to array processing with enhanced degrees of freedom," *IEEE Transactions on Signal Processing*, vol. 58, no. 8, pp. 4167–4181, Aug 2010.

[8] A. Moffet, "Minimum-redundancy linear arrays," *IEEE Transactions on Antennas and Propagation*, vol. 16, no. 2, pp. 172–175, March 1968.

[9] P. P. Vaidyanathan and P. Pal, "Sparse sensing with co-prime samplers and arrays," *IEEE Transactions on Signal Processing*, vol. 59, no. 2, pp. 573–586, Feb 2011.

[10] C. Liu and P. P. Vaidyanathan, "Super nested arrays: Sparse arrays with less mutual coupling than nested arrays," in *2016 IEEE International Conference on Acoustics, Speech and Signal Processing (ICASSP)*, March 2016, pp. 2976–2980.

[11] P. Pal and P. P. Vaidyanathan, "Coprime sampling and the music algorithm," in *2011 Digital Signal Processing and Signal Processing Education Meeting (DSP/SPE)*, Jan 2011, pp. 289–294.

[12] C. Liu and P. P. Vaidyanathan, "High order super nested arrays," in *2016 IEEE Sensor Array and Multichannel Signal Processing Workshop (SAM)*, July 2016, pp. 1–5.

[13] M. Alrmah, S. Weiss, and J. McWhirter, "Implementation of accurate broadband steering vectors for broadband angle of arrival estimation," in *IET Int. Signal Processing Conf. 2013*, Dec 2013, pp. 1–6.

[14] W. Coventry, C. Clemente, and J. Soraghan, "Enhancing Polynomial MUSIC Algorithm for Coherent Broadband Sources Through Spatial Smoothing," in *EUSIPCO 2017*, 2017, pp. 2517–2521.

[15] T.-J. Shan, M. Wax, and T. Kailath, "On spatial smoothing for direction-of-arrival estimation of coherent signals," *IEEE Trans. Acoustics, Speech, and Signal Processing*, vol. 33, no. 4, pp. 806–811, Aug 1985.

[16] W. Coventry, C. Clemente, J. Soraghan, and G. Street, "Polynomial Root-MUSIC Algorithm for Efficient Broadband Direction Of Arrival Estimation."

[17] S. Redif, S. Weiss, and J. G. McWhirter, "Sequential matrix diagonalization algorithms for polynomial evd of parahermitian matrices," *IEEE Trans. Signal Processing*, vol. 63, no. 1, pp. 81–89, Jan 2015.

[18] J. Corr *et al.*, "Multiple shift maximum element sequential matrix diagonalisation for parahermitian matrices," in *2014 IEEE Workshop on Statistical Signal Processing (SSP)*, June 2014, pp. 312–315.

[19] Q. T. Zhang, "Probability of resolution of the music algorithm," *IEEE Transactions on Signal Processing*, vol. 43, no. 4, pp. 978–987, April 1995.